

# MeshLeTemp: Leveraging the Learnable Vertex-Vertex Relationship to Generalize Human Pose and Mesh Reconstruction for In-the-Wild Scenes

Trung Q. Tran, Cuong C. Than, Hai T. Nguyen

*Abstract*—We present MeshLeTemp, a powerful method for 3D human pose and mesh reconstruction from a single image. In terms of human body priors encoding, we propose using a learnable template human mesh instead of a constant template utilized by previous state-of-the-art methods. The proposed learnable template reflects not only vertex-vertex interactions but also the human pose and body shape, being able to adapt to diverse images. We also introduce a strategy to enrich the training data that contains both 2D and 3D annotations. We conduct extensive experiments to show the generalizability of our method and the effectiveness of our data strategy. As one of our ablation studies, we adapt MeshLeTemp to another domain which is 3D hand reconstruction.

## I. INTRODUCTION

Human pose estimation is one of the most vital tasks in computer vision and has been widely used for many real-world applications such as self-driving vehicles, action recognition, or surveillance. When it comes from 2D to 3D human pose estimation, there are many challenges but become more robust to leverage 3D information. As one of the main spirits of 3D human pose estimation, 3D human pose and mesh reconstruction from a single image has received a great deal of attention from the community in recent years. It serves a wide range of applications for human-machine interactions such as motion analysis or virtual reality. Besides the common challenges of human pose estimation such as complex articulation and occlusion, this area also suffers from depth ambiguity [1] and multi-view variation [2].

Reconstructing 3D human pose and mesh from a single image could be categorized into two main approaches. The first approach is referred to as parametric one that aims to predict pose and shape parameters [3], [4], [5], [6], [7], [8]. These methods then use a parametric model like SMPL [9] to generate the 3D human mesh. Since the parametric models incorporate strong prior knowledge about human shape, the parametric approach is robust with a variety of conditions and very little data. Unfortunately, this approach highly depends on the parametric models which are built of particular exemplars. The second approach, a non-parametric one, has emerged as a straightforward yet effective way to directly predict 3D coordinates of human pose and mesh [10], [11], [12]. This paper focuses on elaborating non-parametric methods because the main part of our method is based on non-parametric ones.

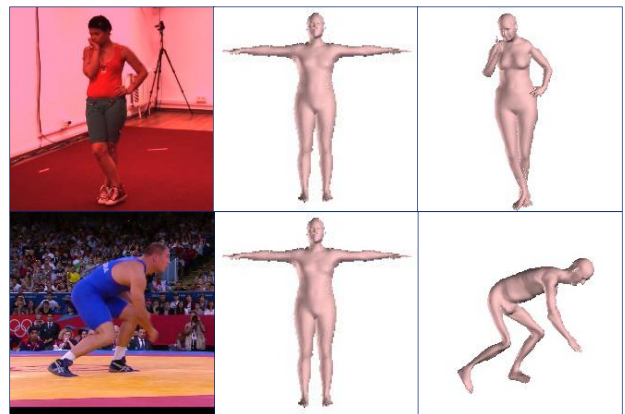


Fig. 1: Illustration of constant and learnable template human mesh (the 2<sup>nd</sup> and 3<sup>rd</sup> column, respectively).

Recently, Graph Convolutional Neural Networks (GCNNs) and Transformers [13] have proven their efficacy in 3D human pose and mesh reconstruction [14], [15], [16]. GraphCMR [14] utilized GCNNs to model local vertex-vertex interactions but did not consider non-local interactions which also have strong correlations. To overcome this limitation, METRO [15] proposed a simple yet effective framework, that utilizes Transformers, to model both local and non-local vertex-vertex interactions. Mesh Graphormer [16] injected graph convolutions into Transformers to further improve local interactions. Both these three methods introduced a template human mesh to preserve the positional information, but only a constant template was used.

In this paper, we propose MeshLeTemp, a multi-layer Transformers-based method leveraging the **learnable** vertex-vertex relationship to effectively reconstruct 3D human pose and mesh. The intuition behind injecting a template human mesh into the image feature is to embed the positional knowledge in the extracted image feature. The constant template might be enough for encoding vertex-vertex connections such as eye-ear or nose-mouth connections. However, it does not reflect the human pose and body shape when feeding different images. We argue that the template human mesh should con-

tain information about not only the vertex-vertex interactions but also the human pose and body shape. We thereby propose leveraging a learnable template human mesh as illustrated in Figure 1. While the constant template is the same for all images, our learnable template is able to adapt to diverse poses of input images. Our experimental results on the in-the-wild dataset, 3DPW, proved the efficacy of the learnable vertex-vertex relationship in learning 3D human pose and mesh. As our understanding, we are the first who utilize the learnable vertex-vertex interactions to support 3D human pose and mesh reconstruction.

Our key contributions are summarized as follows:

- We propose a powerful method, MeshLeTemp, taking the advantage of the learnable template human mesh to reconstruct 3D human pose and mesh effectively.
- MeshLeTemp achieves a better generalization compared to previous state-of-the-art methods.
- To advance the proposed method, we introduce a new dataset that covers various conditions such as occlusion, difficult pose, and nighttime environment.

## II. RELATED WORK

**Human Mesh Reconstruction.** Human mesh reconstruction has attracted the attention of researchers in recent years. The impressive reconstructions could be obtained by using physical devices such as motion cameras [17] or Inertial Measurement Unit (IMU) motion sensors [18]. This approach is costly and even requires complex algorithms to process the sensor’s outputs. Therefore, software-based methods have emerged as a promising approach in this field.

The software-based approach could be divided into two main branches. The first branch utilizes parametric models such as SMPL [9], MANO [19], or STAR [20] to generate the 3D mesh from predicted parameters. This branch takes the advantage of the prior knowledge about human shape incorporated into the parametric models. For instance, [3] proposed an end-to-end way to recover a full 3D human mesh by regressing pose and shape parameters first. They also introduced an additional discriminator network acting as weak supervision to encourage the model to output parameters on the human manifold.

The parametric methods strongly depend on the parametric models and are limited by particular exemplars. Therefore, the second branch of the software-based approach, including non-parametric methods, aims to directly predict the 3D human pose and mesh from a monocular image. [21] proposed a framework that cascades two sub-networks being PoseNet and MeshNet. While PoseNet is responsible for predicting 3D human joints from the input image, MeshNet uses predicted human joints and extracted image features to generate the 3D human mesh. Recently, Graph Convolutional Neural Networks (GCNNs) and Transformers have been leveraged to model both local and global vertex-vertex interactions [14], [15], [16]. Our method leverages Multi-Layer Transformer Encoder for 3D human pose and mesh reconstruction.

**Human Body Priors Encoding.** Encoding human body priors to make 3D human pose and mesh reconstruction more robust is one of the important techniques which has been attractive recently. GraphCMR [14], METRO [15], and Graphormer [16] are the three most relevant studies to our proposed method, which will be presented in Section III. GraphCMR proposed to attach the image feature vector to a 3D template human mesh. This embedded template human mesh was then passed to a series of graph convolutional layers to regress the 3D vertex coordinates. Similarly, METRO obtained positional encoding by concatenating the template human mesh and the image feature. However, instead of using Graph Convolutional Neural Networks (GCNNs), METRO utilized Transformers to model vertex-vertex and vertex-joint interactions. Graphormer is the most recent method which injected graph convolutions into the transformer blocks to make local and global interaction modeling more robust. Additionally, Graphormer extracted the grid features from the last convolutional block of the feature extractor and used it to obtain fine-grained local details.

## III. MESHLETEMP

This section is organized as follows. Section III-A presents the overall framework of MeshLeTemp especially Multi-Layer Transformer Encoder, one of the important parts of our method to predict the 3D human joints and mesh simultaneously. Next, Section III-B describes our proposed block to learn the template human mesh. As one of our contributions, Section III-C shows our approach to train MeshLeTemp with both public datasets and real-world data. Finally, Section III-D presents our training details.

### A. Overall Framework

The overall framework of MeshLeTemp is illustrated in Figure 2. Our model consists of two main parts. While the first part uses a Convolutional Neural Network (CNN) to extract the image feature vector, the second one is responsible for generating 3D human joints and mesh by utilizing a Multi-Layer Transformer Encoder (MTE). We leverage HRNets architecture [22], an existing large-scale network, for extracting the image features. HRNets have been proven to be a powerful architecture in visual recognition.

The output of Convolutional Neural Network (CNN) is 2048 feature maps with the size of  $7 \times 7$  each. Inside the tokenizer, a 1D CNN is used to tokenize the image feature into 2048-feature vectors for 445 points where each point is either joint or vertex. In another word, each point either joint or vertex consists of 2048 features extracted by CNN. Tokenizer also takes the output of the template learner, which contains the 3D coordinates  $(x_i, y_i, z_i)$  of the  $i^{th}$  body vertex. Tokenizer finally outputs 445 queries where each query is a 2051-dimensional vector (2048 image features and 3 vertex coordinates). More details about the template learner will be presented in Section III-B.

As illustrated in Figure 2, Multi-Layer Transformer Encoder (MTE) takes as input joint queries and vertex queries. For

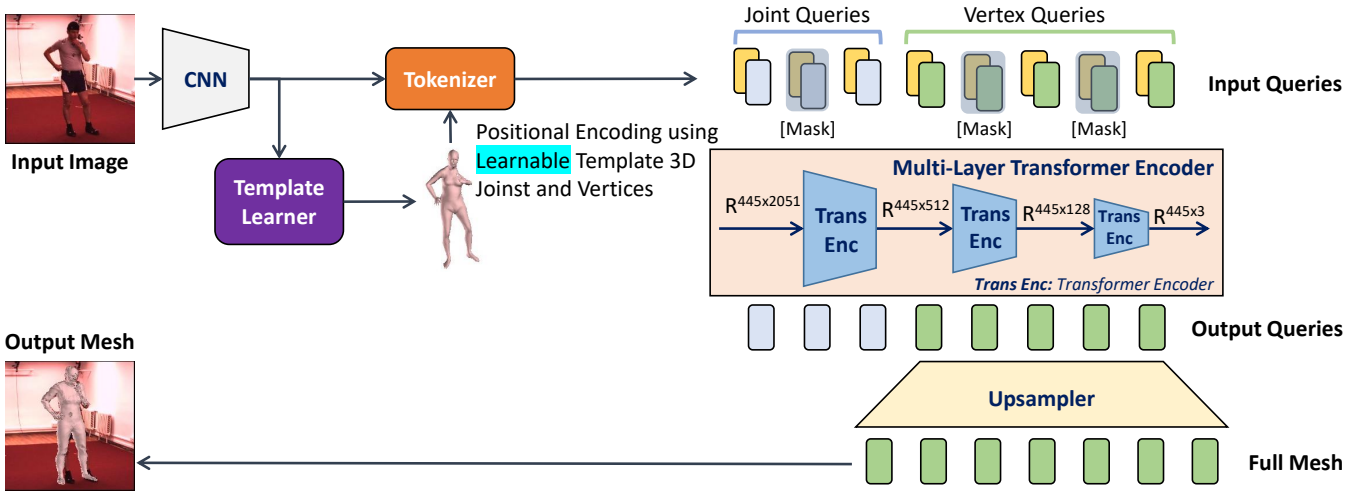


Fig. 2: MeshLeTemp for 3D Human Mesh Reconstruction. Our framework first uses a feature extractor which is a Convolutional Neural Network (CNN) to extract the image feature. This image feature is fed into a template learner to obtain the template human mesh. The learnable template mesh and the extracted image feature are then combined into a set of joint queries and vertex queries. Finally, a Multi-Layer Transformer Encoder takes as input the set of queries to reconstruct the 3D human pose and mesh.

joint queries, we train our model with 14 keypoints which in order are right ankle, right knee, right hip, left hip, left knee, left ankle, right wrist, right elbow, right shoulder, left shoulder, left elbow, left wrist, neck, head. For vertex queries, as recommended by [15] and [16], we use a coarse human mesh, containing 431 vertices, to make the training faster. MTE consists of three transformer encoder blocks with dimensionality gradually reduced. The output of MTE includes 3D coordinates for 431 vertices and 14 keypoints. At the end of the framework, MeshLeTemp upsamples the predicted coarse mesh to the original human mesh (6890 vertices) by using learnable Multi-Layer Perceptions (MLPs). To take occlusions into account, we utilize Masked Vertex Modeling (MVM) which was successfully used by METRO [15]. MVM masks some percentages of the input queries randomly. Instead of recovering the masked inputs as done by Masked Language Modeling (MLM) [23], MTE is asked to regress all the joints and vertices.

### B. Learnable Template Human Mesh

In the same spirit as positional encoding [24], [14], [15], [16], we utilize a template human mesh to preserve the positional information of vertex-vertex interactions. Previous works used a constant template which is the same for all input images. As a result, this positional encoding does not reflect the human pose and body shape. For example, the standing pose and bowing pose will use the same template human mesh, as described in Figure 1.

We argue that it would be beneficial if we also consider the human pose and body shape for positional encoding. We thereby propose an extra block, called Template Learner (TL), to learn the template human mesh from the corresponding

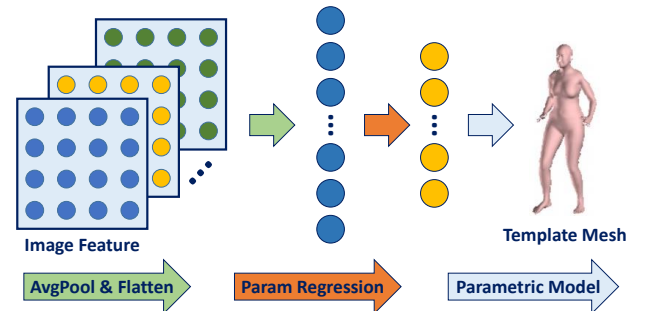


Fig. 3: Procedure of learning template human mesh.

image feature, as illustrated in Figure 3. The extracted image feature goes through an Average Pooling layer and is then flattened to a 1D vector. At the heart of Template Learner, we use Multi-Layer Perceptions (MLPs) layers to regress the body and shape parameters. These parameters are then fed into a parametric model, which is SMPL [9] in our work, to obtain the learnable template human mesh. The proposed learnable template is robust with various input images, and its efficacy will be clarified in Section IV.

### C. Mix-Training with Real-World Data

To improve the generalizability of our model, we introduce a data strategy (Figure 4) to leverage real-world data taken from any camera.

We need to have both 2D and 3D information for the training data. As shown in Figure 4, the 2D keypoints are manually annotated by us. For 3D information, we utilize

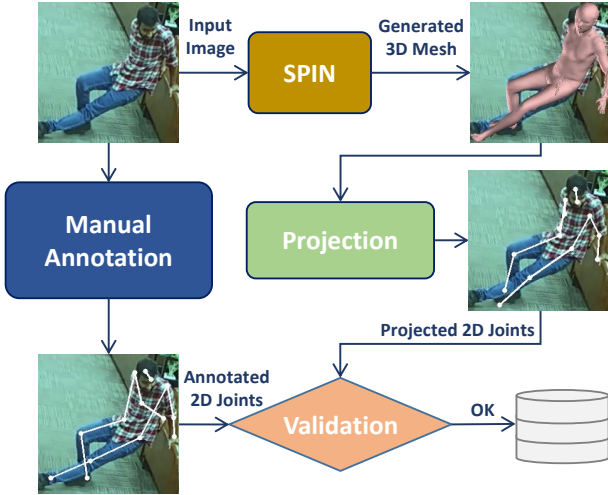


Fig. 4: Proposed data strategy.

SPIN [7] to generate the 3D human mesh from the given image. This generated mesh is then fed into a projection algorithm to obtain the projected 2D keypoints. Because the quality of 3D human mesh depends on the performance of SPIN model, we need to ignore the bad-quality meshes. To do so, we compare the annotated with projected 2D keypoints and use a threshold to filter the unreasonable meshes. As a result, there are more than 35K images having only 2D keypoints and more than 23K images having both 2D keypoints and 3D mesh out of more than 58K images created by us.

#### D. Training Details

We use a similar training strategy as used in METRO [15]. Concretely, we use  $L_1$  loss for both predicted 3D vertices and predicted 3D joints, leading to  $\mathcal{L}_V$  and  $\mathcal{L}_J$  respectively. Notably, the 3D joints can be obtained from the predicted 3D vertices by using a pre-defined regression matrix  $G \in \mathbb{R}^{K \times M}$ , as shown in the literature [3], [14], [25], where  $K$  is the number of joints and  $M$  is the number of vertices of a person. Therefore, we also use  $L_1$  loss for these regressed 3D joints, resulting in  $\mathcal{L}_J^{reg}$ . On top of the outputs of the model, we use Multi-Layer Perceptions (MLPs) layers to learn the camera parameters, which are used to project the 3D joints to the 2D space.  $L_1$  loss is used for these projected 2D joints, leading to  $\mathcal{L}_J^{proj}$ .

Different from previous methods using the constant template human mesh, we additionally utilize  $L_1$  loss to supervise the learnable template which is built out of 3D vertices, resulting in  $\mathcal{L}_V^{temp}$ . Our overall objective function is formulated as follows:

$$\mathcal{L} = \alpha \times (\mathcal{L}_V + \mathcal{L}_J + \mathcal{L}_J^{reg} + \mathcal{L}_V^{temp}) + \beta \times \mathcal{L}_J^{proj}, \quad (1)$$

where  $\alpha$  and  $\beta$  are to indicate the availability of 3D and 2D ground-truths, respectively.

We train MeshLeTemp with the Adam optimizer [26] and cosine learning rate scheduler [27]. Given a base learning

rate  $\eta$ , the learning rate at the training step  $s$  is set to  $\eta \times \cos \frac{7\pi s}{16S}$ , where  $S$  is the total number of training steps. In our experiments, we use a base learning rate of  $1e-4$  and train our model for 50 epochs. Notably, our training is much faster than the two most relevant methods, METRO [15] and Graphormer [16], which trained their models for 200 epochs.

## IV. EXPERIMENTAL RESULTS

This section presents the efficacy of our MeshLeTemp, especially the learnable template human mesh. Our main results are reported in Section IV-B, showing the performance comparison of our method with other state-of-the-art methods. Section IV-C describes our qualitative results compared to METRO and Graphormer. Finally, we conduct the ablation study (Section IV-D) to show the effectiveness of our data strategy and learnable template. We also demonstrate the generalizability of MeshLeTemp on 3D hand reconstruction.

### A. Datasets

We conduct extensive experiments with mix-training using 3D and 2D data. Each dataset is described as follows.

**Human3.6M** [17] is an indoor and large-scale dataset containing accurate 3D human poses in natural environments. Each image is acquired by recording the performance of 5 female and 6 male subjects under 4 different viewpoints, resulting in 3.6M images in total. The ground-truth 3D mesh is inaccessible due to the license issue. Therefore, we use the pseudo-labels generated by SMPLify-X [28]. As the common setting, we use the subjects S1, S5, S6, S7, and S8 for training, and keep the subjects S9 and S11 for testing.

**UP-3D** [29] is a synthesized outdoor dataset, created by fitting the SMPLify [30] to generate the ground-truth 3D annotations. We use this dataset only for training.

**MuCo-3DHP** [31] is a synthesized dataset generated by compositing the training images of MPIINF-3DHP [32] with various real-world background images. MuCo-3DHP consists of 200K images, and half of them have augmented backgrounds.

**COCO** [33] is a large-scale dataset for 2D human pose estimation, containing 65K images for training, 5K images for validation, and 15K images for testing. The 3D annotations are not provided, so we use the pseudo-3D mesh generated by SMPLify-X [28], as provided in [7].

**MPII** [34] is an outdoor dataset with 2D human poses, including 14K images for training. We use this dataset only for training.

**3DPW** [18] is the first in-the-wild dataset for accurate 3D human pose estimation. 3DPW contains 60 video sequences with 22K images for training and 35K images for testing. For a fair comparison with previous state-of-the-art methods, we also conduct our experiments by training our model on the 3DPW training set and use the same evaluation metrics as Human3.6M.

**FreiHAND** [35] is a 3D hand dataset with provided MANO-based 3D hand annotations. This dataset has 130K images for training and 14K images for testing, acquired by recording

TABLE I: Comparisons with the two most relevant methods on Human3.6M and 3DPW dataset. All models are trained on the same set of datasets. The results of METRO and Graphormer are reproduced by us using the provided checkpoints.

METHOD	HUMAN3.6M		3DPW VAL			3DPW TEST		
	MPJPE ↓	PA-MPJPE ↓	MPVE ↓	MPJPE ↓	PA-MPJPE ↓	MPVE ↓	MPJPE ↓	PA-MPJPE ↓
MODELS ARE NOT FINE-TUNED ON 3DPW TRAINING SET								
METRO	54.0	36.8	127.5	112.4	71.0	130.2	114.3	67.2
GRAPHORMER	<b>51.2</b>	<b>34.6</b>	147.6	131.1	86.7	157.6	142.2	88.0
MESHLETEMP	56.8	37.6	<b>118.3</b>	<b>102.0</b>	<b>66.0</b>	<b>123.4</b>	<b>106.0</b>	<b>62.8</b>
MODELS ARE FINE-TUNED ON 3DPW TRAINING SET								
METRO	78.6	48.9	79.6	65.9	45.0	88.3	77.1	47.9
GRAPHORMER	76.1	47.6	77.6	<b>63.0</b>	<b>42.0</b>	<b>87.7</b>	<b>74.7</b>	<b>45.6</b>
MESHLETEMP	<b>75.6</b>	<b>47.4</b>	<b>77.4</b>	64.5	44.8	88.6	76.8	47.6

different hand actions performed by 32 people. We conduct our experiments on the training set and perform the evaluation on their online server.

**Real-world data** is generated by us using the strategy proposed in Section III-C. There are more than 58K images of which 35K have only 2D annotations and 23K have both 2D and 3D annotations. Some examples of our generated data are described in Figure 5. As presented in Section III-C, the generated data is examined and could be eliminated if having the bad quality. As a result, the image in the top row of Figure 5 will be ignored from our dataset because it has the bad generated 3D mesh, leading to the unreasonable projected 2D joints.



Fig. 5: Examples of our data. The left side is projected 2D joints, and the right side is for generated 3D mesh.

### B. Main Results

We check the generalizability of our model by comparing it with the two most relevant methods, METRO [15] and Graphormer [16], as shown in Table I. For a fair comparison, we train our model on the same datasets used in METRO and Graphormer. Specifically, we train our model using the mix-training strategy which uses both 3D and 2D training data. Our training dataset includes Human3.6M, UP-3D, MuCo-3DHP, COCO, and MPII. As shown in the top part of Table I, MeshLeTemp achieves much better performance on 3DPW validation and test set compared to METRO and Graphormer. For instance, MeshLeTemp improves MPVE by 9.2 and 29.3 points on 3DPW validation set compared to METRO and Graphormer respectively. On 3DPW test set, MeshLeTemp obtains PA-MPJPE improvement of 4.4 and 25.2 points compared to METRO and Graphormer respectively. Notably, 3DPW is an in-the-wild dataset containing outdoor images, so our MeshLeTemp achieves a much better generalization compared to METRO and Graphormer.

However, without fine-tuning on 3DPW training set, MeshLeTemp has worse performance than METRO and Graphormer on Human3.6M. To further investigate this, we fine-tune our model on 3DPW training set, which is similar to other methods. The results of fine-tuned models are shown in the bottom part of Table I. After fine-tuning on 3DPW training set, MeshLeTemp obtains comparable performance with METRO and Graphormer. Especially, MeshLeTemp still achieves better results compared to METRO in most metrics. Notably, MeshLeTemp obtains the best results on Human3.6M (improving MPJPE by 3.0 points and PA-MPJPE by 1.5 points compared to METRO), consolidating the generalizability of our method.

We also compare MeshLeTemp with other state-of-the-art methods, as shown in Table II. Notably, when conducting the comparisons on 3DPW dataset, we fine-tune our model on 3DPW training set, as similar to other methods. The results show that MeshLeTemp strongly outperforms previous state-of-the-art methods. Additionally, we utilize the real-world data obtained by the strategy proposed in Section III-C to train

TABLE II: Comparisons with other state-of-the-art methods on Human3.6M and 3DPW dataset. \* denotes the results cited from METRO. † means our proposed data is used.

METHOD	HUMAN3.6M		3DPW TEST		
	MPJPE ↓	PA-MPJPE ↓	MPVE ↓	MPJPE ↓	PA-MPJPE ↓
HMR [3]	-	56.8	-	-	81.3*
GRAPHCMR [14]	-	50.1	-	-	70.2*
SPIN [7]	-	41.1	-	-	59.2
POSE2MESH [25]	64.9	46.3	105.3	89.5	56.3
I2LMESHNET [21]	55.7	41.7	-	93.2	57.7
VIBE [4]	65.9	41.5	99.1	83.0	52.0
MESHLETEMP (OURS)	56.8	37.6	88.6	76.8	47.6
MESHLETEMP <sup>†</sup> (OURS)	<b>54.9</b>	<b>37.0</b>	<b>86.5</b>	<b>74.8</b>	<b>46.8</b>

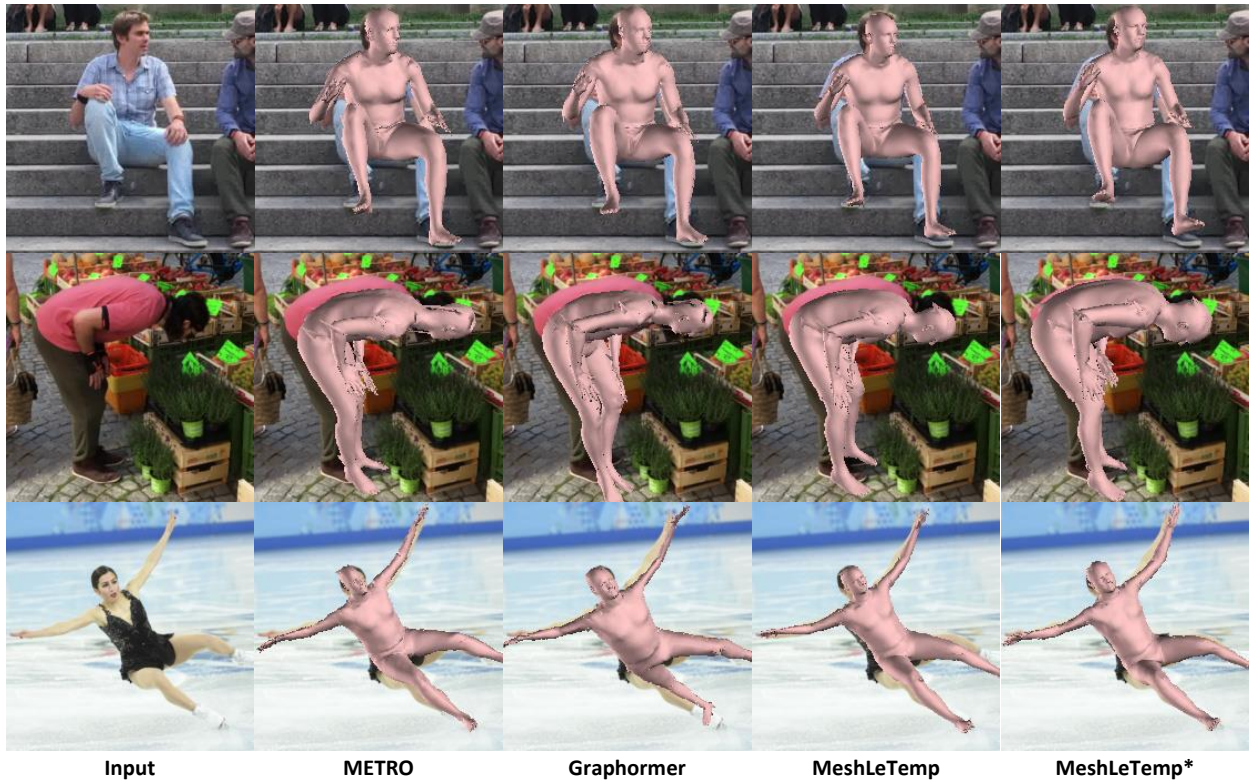


Fig. 6: Qualitative results of the methods on in-the-wild datasets. The top two rows are the results of 3DPW test set, and the bottom row is the result from another source. All models are not fine-tuned on 3DPW training data. \* means our proposed data is used.

our model. MeshLeTemp with our extra data still outperforms other methods. For instance, MeshLeTemp with our extra data reduces PA-MPJPE by 4.5 and 5.2 points compared to VIBE on Human3.6M and 3DPW test set, respectively. The results also show the efficacy of our data strategy, which will be clarified in Section IV-D.

### C. Qualitative Results

Figure 6 shows the qualitative results of our MeshLeTemp compared to the two most relevant methods, METRO and Graphormer. We evaluate the models on in-the-wild images to

check the generalizability of the methods. The top two rows are the results of 3DPW test set, and the bottom row shows the result of the image obtained from the Internet.

- For the simple case where the background is not complicated, all methods give acceptable results as illustrated in the top row of Figure 6.
- However, for the hard background as shown in the middle row of Figure 6, MeshLeTemp outperforms METRO and Graphormer. Both METRO and Graphormer are failed to fit the reconstructed 3D mesh to the person (the backbone

TABLE III: Ablation study with our proposed dataset. <sup>†</sup> means our proposed data is used.

METHOD	HUMAN3.6M		3DPW VAL			3DPW TEST		
	MPJPE ↓	PA-MPJPE ↓	MPVE ↓	MPJPE ↓	PA-MPJPE ↓	MPVE ↓	MPJPE ↓	PA-MPJPE ↓
MODELS ARE NOT FINE-TUNED ON 3DPW TRAINING SET								
MESHLETEMP	56.8	37.6	118.3	102.0	66.0	123.4	106.0	62.8
MESHLETEMP <sup>†</sup>	<b>54.9</b>	<b>37.0</b>	<b>112.0</b>	<b>100.9</b>	<b>64.0</b>	<b>110.2</b>	<b>101.3</b>	<b>62.1</b>
MODELS ARE FINE-TUNED ON 3DPW TRAINING SET								
MESHLETEMP	<b>75.6</b>	<b>47.4</b>	77.4	64.5	44.8	88.6	76.8	47.6
MESHLETEMP <sup>†</sup>	75.8	48.8	<b>76.4</b>	<b>63.7</b>	<b>43.5</b>	<b>86.5</b>	<b>74.8</b>	<b>46.8</b>

deviates, and the body shape is not matched). Otherwise, MeshLeTemp obtains a more reasonable reconstruction of 3D mesh. Especially, MeshLeTemp with our extra data can fit the reconstructed 3D mesh to the person well.

- The bottom row of Figure 6 describes the case of the hard pose. Graphormer gives the worst result, where the right leg is weird. The other three models obtain acceptable results. However, when we carefully look at the predicted 3D meshes, MeshLeTemp has the more sophisticated result, where the head is more fine-grained than that of METRO.

#### D. Ablation Study

**Effectiveness of Proposed Data Strategy.** We first conduct the ablation study to check if our proposed data is effective, as shown in Table III. Without fine-tuning on 3DPW training set, using our extra data gives better results in all cases. When fine-tuning on 3DPW training set, MeshLeTemp with our extra data does not improve the results on Human3.6M. The main reason is that 3DPW is an outdoor dataset while Human3.6M is an indoor dataset. Fine-tuning on 3DPW dataset might lead to performance reduced on an indoor dataset. However, this degradation is not significant in our MeshLeTemp while the good performance on the target dataset, 3DPW, is still obtained.

**Learnable Template Supervision.** As mentioned in Section III-D, we use  $L_1$  loss to supervise the learnable template human mesh. Table IV shows the comparison between supervising and not supervising the learnable template during the training process. The results show that supervising the learnable template helps the model become more robust in reconstructing 3D human pose and mesh.

TABLE IV: Analysis of supervising the learnable template human mesh on 3DPW test set.

METHOD	MPVE ↓	MPJPE ↓	PA-MPJPE ↓
NO SUPERVISION	114.8	103.5	63.0
SUPERVISION	<b>110.2</b>	<b>101.3</b>	<b>62.1</b>

**Training Progress.** To clarify the effectiveness of applying the learnable template, we observe the model performance

during the training process, as shown in Figure 7. At the 10 first epochs, we use the constant template. We switch to using the learnable template from the 10<sup>th</sup> epoch. As shown in Figure 7, the errors are significantly reduced when using the learnable template. As a result, our training process only needs to take 50 epochs while the previous methods (METRO and Graphormer) need 200 training epochs; this proves that our method has a faster training compared to the two most relevant methods, METRO and Graphormer.

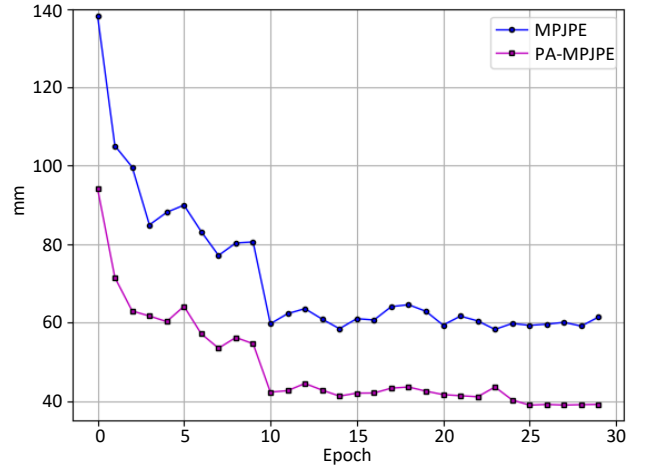


Fig. 7: Performance of MeshLeTemp during the training process. The metrics are measured on Human3.6M. The learnable template is applied from the 10<sup>th</sup> epoch.

**Progress of Learnable Template Human Mesh.** We observe the learnable template during the training process to see how the template human mesh grows up, as illustrated in Figure 8. The top row depicts the predicted 2D keypoints, and the bottom row is for the learned 3D template human mesh.

- At the first iterations (the 1<sup>st</sup> column for instance), the mesh templates are quite similar among images.
- When the training progresses, the template starts to fit the specific images but is still poor at hard poses (the 2<sup>nd</sup> and 3<sup>rd</sup> column).
- Finally, the visualization in the 4<sup>th</sup> and 5<sup>th</sup> column shows that the template human mesh tries to handle the hard

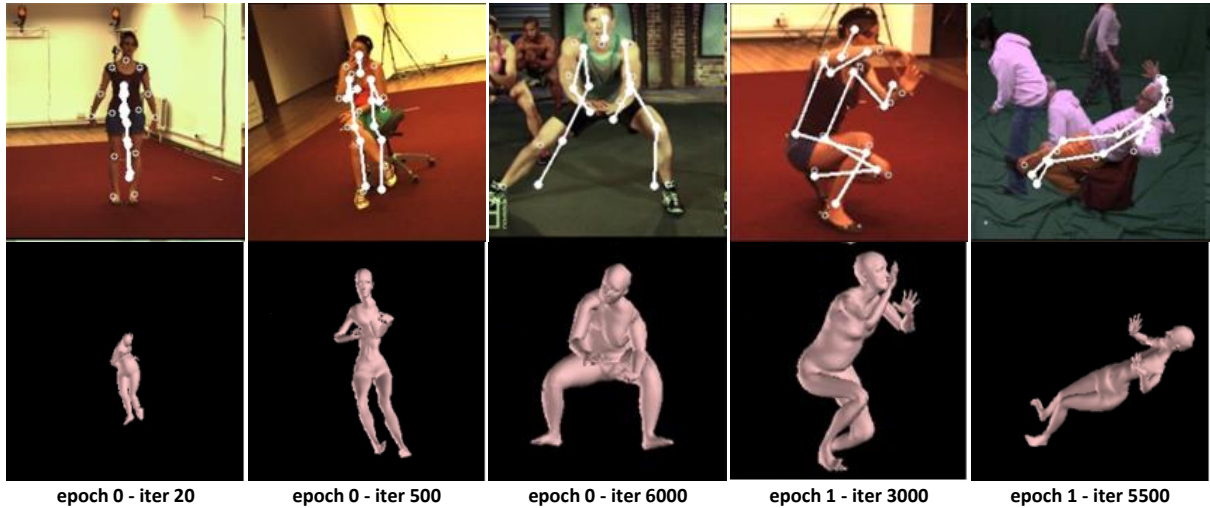


Fig. 8: Illustration of the learnable template human mesh during the training process.



Fig. 9: Qualitative results of our method on in-the-wild hand datasets. The top two rows are from FreiHAND test set. The bottom row is our collected data.

poses.

**Generalization to 3D Hand Reconstruction.** We evaluate our learnable template on 3D hand reconstruction, as shown in Figure 9.

- For simple cases, our method performs well when accurately reconstructing 3D hand mesh, as shown in the top row of Figure 9.
- The middle row of Figure 9 includes the cases where the hand is holding something. Our method still can give the reasonable reconstruction.
- To inspect the generalizability of our method, we also

prepare some testing images as illustrated in the bottom row of Figure 9. The results show that MeshLeTemp is able to adapt to unseen in-the-wild scenarios even in the hard case (the bottom-right sample).

## V. CONCLUSION

We introduce a powerful method to effectively encode the human body priors into the image feature. Instead of using the constant template human mesh as previous methods did, our method, MeshLeTemp, leverages the learnable template to reconstruct 3D human pose and mesh from a single input

image. The extensive experiments show that our method obtains the better generalization compared to previous state-of-the-art methods. To advance the performance, we propose a data strategy to create real-world data containing both 2D and 3D annotations. The results also show that our extra data helps improve the performance of our model. For future work, we are interested in elaborately adapting our method to another domain such as 3D hand reconstruction.

## REFERENCES

- [1] C. Li and G. H. Lee, "Generating multiple hypotheses for 3d human pose estimation with mixture density network," in *Proceedings of the IEEE/CVF Conference on Computer Vision and Pattern Recognition*, 2019, pp. 9887–9895.
- [2] J. Dong, W. Jiang, Q. Huang, H. Bao, and X. Zhou, "Fast and robust multi-person 3d pose estimation from multiple views," in *Proceedings of the IEEE/CVF Conference on Computer Vision and Pattern Recognition*, 2019, pp. 7792–7801.
- [3] A. Kanazawa, M. J. Black, D. W. Jacobs, and J. Malik, "End-to-end recovery of human shape and pose," in *Proceedings of the IEEE conference on computer vision and pattern recognition*, 2018, pp. 7122–7131.
- [4] M. Kocabas, N. Athanasiou, and M. J. Black, "Vibe: Video inference for human body pose and shape estimation," in *Proceedings of the IEEE/CVF Conference on Computer Vision and Pattern Recognition*, 2020, pp. 5253–5263.
- [5] G. Pavlakos, L. Zhu, X. Zhou, and K. Daniilidis, "Learning to estimate 3d human pose and shape from a single color image," in *Proceedings of the IEEE Conference on Computer Vision and Pattern Recognition*, 2018, pp. 459–468.
- [6] M. Omran, C. Lassner, G. Pons-Moll, P. Gehler, and B. Schiele, "Neural body fitting: Unifying deep learning and model based human pose and shape estimation," in *2018 international conference on 3D vision (3DV)*. IEEE, 2018, pp. 484–494.
- [7] N. Kolotouros, G. Pavlakos, M. J. Black, and K. Daniilidis, "Learning to reconstruct 3d human pose and shape via model-fitting in the loop," in *Proceedings of the IEEE/CVF International Conference on Computer Vision*, 2019, pp. 2252–2261.
- [8] Y. Rong, Z. Liu, C. Li, K. Cao, and C. C. Loy, "Delving deep into hybrid annotations for 3d human recovery in the wild," in *Proceedings of the IEEE/CVF International Conference on Computer Vision*, 2019, pp. 5340–5348.
- [9] M. Loper, N. Mahmood, J. Romero, G. Pons-Moll, and M. J. Black, "Smpl: A skinned multi-person linear model," *ACM transactions on graphics (TOG)*, vol. 34, no. 6, pp. 1–16, 2015.
- [10] G. Pavlakos, X. Zhou, K. G. Derpanis, and K. Daniilidis, "Coarse-to-fine volumetric prediction for single-image 3d human pose," in *Proceedings of the IEEE conference on computer vision and pattern recognition*, 2017, pp. 7025–7034.
- [11] X. Sun, B. Xiao, F. Wei, S. Liang, and Y. Wei, "Integral human pose regression," in *Proceedings of the European Conference on Computer Vision (ECCV)*, 2018, pp. 529–545.
- [12] X. Zhou, Q. Huang, X. Sun, X. Xue, and Y. Wei, "Towards 3d human pose estimation in the wild: a weakly-supervised approach," in *Proceedings of the IEEE International Conference on Computer Vision*, 2017, pp. 398–407.
- [13] A. Vaswani, N. Shazeer, N. Parmar, J. Uszkoreit, L. Jones, A. N. Gomez, Ł. Kaiser, and I. Polosukhin, "Attention is all you need," in *Advances in neural information processing systems*, 2017, pp. 5998–6008.
- [14] N. Kolotouros, G. Pavlakos, and K. Daniilidis, "Convolutional mesh regression for single-image human shape reconstruction," in *Proceedings of the IEEE/CVF Conference on Computer Vision and Pattern Recognition*, 2019, pp. 4501–4510.
- [15] K. Lin, L. Wang, and Z. Liu, "End-to-end human pose and mesh reconstruction with transformers," in *Proceedings of the IEEE/CVF Conference on Computer Vision and Pattern Recognition*, 2021, pp. 1954–1963.
- [16] —, "Mesh graphormer," *arXiv preprint arXiv:2104.00272*, 2021.
- [17] C. Ionescu, D. Papava, V. Olaru, and C. Sminchisescu, "Human3.6m: Large scale datasets and predictive methods for 3d human sensing in natural environments," *IEEE transactions on pattern analysis and machine intelligence*, vol. 36, no. 7, pp. 1325–1339, 2013.
- [18] T. von Marcard, R. Henschel, M. J. Black, B. Rosenhahn, and G. Pons-Moll, "Recovering accurate 3d human pose in the wild using imus and a moving camera," in *Proceedings of the European Conference on Computer Vision (ECCV)*, 2018, pp. 601–617.
- [19] J. Romero, D. Tzionas, and M. J. Black, "Embodied hands: Modeling and capturing hands and bodies together," *ACM Transactions on Graphics (ToG)*, vol. 36, no. 6, pp. 1–17, 2017.
- [20] A. A. Osman, T. Bolkart, and M. J. Black, "Star: Sparse trained articulated human body regressor," in *Computer Vision—ECCV 2020: 16th European Conference, Glasgow, UK, August 23–28, 2020, Proceedings, Part VI 16*. Springer, 2020, pp. 598–613.
- [21] G. Moon and K. M. Lee, "I2l-meshnet: Image-to-lixel prediction network for accurate 3d human pose and mesh estimation from a single rgb image," in *Computer Vision—ECCV 2020: 16th European Conference, Glasgow, UK, August 23–28, 2020, Proceedings, Part VII 16*. Springer, 2020, pp. 752–768.
- [22] J. Wang, K. Sun, T. Cheng, B. Jiang, C. Deng, Y. Zhao, D. Liu, Y. Mu, M. Tan, X. Wang *et al.*, "Deep high-resolution representation learning for visual recognition," *IEEE transactions on pattern analysis and machine intelligence*, 2020.
- [23] J. Devlin, M.-W. Chang, K. Lee, and K. Toutanova, "Bert: Pre-training of deep bidirectional transformers for language understanding," *arXiv preprint arXiv:1810.04805*, 2018.
- [24] T. Groueix, M. Fisher, V. G. Kim, B. C. Russell, and M. Aubry, "3d-coded: 3d correspondences by deep deformation," in *Proceedings of the European Conference on Computer Vision (ECCV)*, 2018, pp. 230–246.
- [25] H. Choi, G. Moon, and K. M. Lee, "Pose2mesh: Graph convolutional network for 3d human pose and mesh recovery from a 2d human pose," in *European Conference on Computer Vision*. Springer, 2020, pp. 769–787.
- [26] D. P. Kingma and J. Ba, "Adam: A method for stochastic optimization," *arXiv preprint arXiv:1412.6980*, 2014.
- [27] I. Loshchilov and F. Hutter, "Sgdr: Stochastic gradient descent with warm restarts," *arXiv preprint arXiv:1608.03983*, 2016.
- [28] G. Pavlakos, V. Choutas, N. Ghorbani, T. Bolkart, A. A. Osman, D. Tzionas, and M. J. Black, "Expressive body capture: 3d hands, face, and body from a single image," in *Proceedings of the IEEE/CVF Conference on Computer Vision and Pattern Recognition*, 2019, pp. 10 975–10 985.
- [29] C. Lassner, J. Romero, M. Kiefel, F. Bogo, M. J. Black, and P. V. Gehler, "Unite the people: Closing the loop between 3d and 2d human representations," in *Proceedings of the IEEE conference on computer vision and pattern recognition*, 2017, pp. 6050–6059.
- [30] F. Bogo, A. Kanazawa, C. Lassner, P. Gehler, J. Romero, and M. J. Black, "Keep it smpl: Automatic estimation of 3d human pose and shape from a single image," in *European conference on computer vision*. Springer, 2016, pp. 561–578.
- [31] D. Mehta, O. Sotnychenko, F. Mueller, W. Xu, S. Sridhar, G. Pons-Moll, and C. Theobalt, "Single-shot multi-person 3d pose estimation from monocular rgb," in *2018 International Conference on 3D Vision (3DV)*. IEEE, 2018, pp. 120–130.
- [32] D. Mehta, H. Rhodin, D. Casas, P. Fua, O. Sotnychenko, W. Xu, and C. Theobalt, "Monocular 3d human pose estimation in the wild using improved cnn supervision," in *2017 international conference on 3D vision (3DV)*. IEEE, 2017, pp. 506–516.
- [33] T.-Y. Lin, M. Maire, S. Belongie, P. Hays, P. Perona, D. Ramanan, P. Dollár, and C. L. Zitnick, "Microsoft coco: Common objects in context," in *European conference on computer vision*. Springer, 2014, pp. 740–755.
- [34] M. Andriluka, L. Pishchulin, P. Gehler, and B. Schiele, "2d human pose estimation: New benchmark and state of the art analysis," in *Proceedings of the IEEE Conference on Computer Vision and Pattern Recognition*, 2014, pp. 3686–3693.
- [35] C. Zimmermann, D. Ceylan, J. Yang, B. Russell, M. Argus, and T. Brox, "Freihand: A dataset for markerless capture of hand pose and shape from single rgb images," in *Proceedings of the IEEE/CVF International Conference on Computer Vision*, 2019, pp. 813–822.